Performance of geogrid reinforced and stabilized base courses

Lars Vollmert
NAUE GmbH & Co. KG, Germany

Gerhard Bräu
Zentrum Geotechnik, Technical University of Munich, Germany

ABSTRACT: Unbound base courses are subject to high cyclic-dynamic stresses resulting from traffic loads. As they cannot absorb tensile forces, they can be reinforced if necessary. Field experiences have shown that the use of geosynthetics improves the trafficability of unpaved roads on soft subsoil. Specifically, the thickness of the base course and therefore the amount of high-quality geomaterials, e.g. crushed gravel, can be reduced. There are extensive studies throughout the literature that confirm the mechanism of the bearing capacity improvement, concentrating on individual effects such as the influence of the bearing layer thickness at constant subsoil strength. To clarify the influence of the reinforcement and to investigate the effectiveness of different geosynthetics in unpaved roads, field measurements, systematic laboratory as well large-scale tests and cyclic triaxial tests were carried out. Beside the bearing strength and stiffness of the soft subsoil, the base course thickness as well as the type, and hence the tensile and structural stiffness have been found to dominate (beside the granular material itself) the overall behavior of the stabilized base course material. Under the identified stress and deformation conditions, controlled tests show that the reinforcement reduces the plastic deformations by more than 30 % and thus influences the serviceability significantly.

Keywords: geogrid, reinforcement, stabilization, cyclic loading, serviceability

1 INTRODUCTION

In roads, unbound base courses of the superstructure are an essential part of the total construction. They are subject to high cyclic-dynamic stresses resulting from traffic loads. Due to the specific superstructure distributing the loads, the resulting shear and bending stresses are reduced to an acceptable range of vertical and horizontal stress. The highest absolute stresses clearly occur in weak and low subbase with less rigid, bound cover layers. The relations between vertical and horizontal stresses, which are furthermore decisive for the loads and horizontal strains of the unbound base courses, are usually in the range of σ_V/σ_H = 2 / 15. Under unfavorable conditions and weakly dimensioned structures, however, they can increase significantly by the power of ten up to approx. σ_V/σ_H = 150.

As unbound base courses cannot absorb tensile forces, they are – depending on the application – reinforced by geogrid layers. Especially for the case when the base course thickness is to be reduced in combination with varying thicknesses of the asphalt layers (for example in municipal road construction) or is reduced anyway in case of subordinated construction classes, or if the asphalt base course is missing completely, the unbound base course has a crucial importance. The same applies for increasing loads. Numrich (2003) points out that, in practice, permitted axle loads of usually 12 t are exceeded by up to 50 %. The additional stresses are correspondingly high and lead to an early damage of the pavement structures.

Logically, the bearing capacity of unpaved roads is mainly influenced by the type of material used for the base course, the thickness, the kind of installation and its compaction as well as the strength of the subsoil. Positive benefit has been documented by applying geogrids with high tensile stiffness to the structure, absorbing tensile forces. Thus, the interaction between the subsoil, geotextile reinforcement and the base course becomes of additional importance.

In the literature a plethora of tests is documented. In most of the test series either boundary conditions were not clearly described or only particular geotextile products were examined. Moreover, in the experimental approach, by far too many influencing parameters were varied within a single test series and therefore results do not allow to find a suitable theoretical design model.

Since decades, the effect of geosynthetics is subject to international and national scientific investigation and the application of geosynthetics is observed with a critical eye. In the large number of publications and the sometimes regionally strengthened state of knowledge, separating and restrictive characteristics are often underlined more strongly than parallels.

Intensive efforts of the industry (Schwerdt et al. 2004; van Gurp & Westera 2008) have documented the benefit of the reinforcement, but differentiation of effects is covered by systematic test problems. Some of the studies, e.g. Cuelho & Perkins (2009) and Cuehlo et al. (2014), well prepared and documented, were not able to identify the effect of filter stability and separation effects and thus clear results concerning tensile stiffness and interaction are covered by mixing up effects and misinterpretation from practitioners.

Nevertheless, in previously carried out research, some of the main influencing parameters controlling the effectiveness of geosynthetics in unpaved roads were examined in detail, e.g. by Bräu & Vogt 2011 (in English documented by Bräu & Vogt 2018) and Vollmert 2016 (summed up and added by additional information by Vollmert et al. 2017). This paper gives a brief overview of some of the tests and results, contributing to enhance the understanding of the effect of geosynthetic reinforcement on base course stabilization, making use of the strength-strain-characteristic of the geogrid, thus by definition of reinforcement.

2 MECHANICAL INTERACTION OF SOIL AND REINFORCEMENT

For the understanding of the function, and lateron its effects on the use of unbound base courses – for small as well as for large deformations – the interaction between reinforcement and soil is decisive.

The resistance of a geogrid to displacements in the ground is composed of friction parts and earth resistance parts. The earth resistance, mobilized in front of crossing elements, leads to a significant modification of the strain and stabilizing ratio of the grain structure and can grow to more than 50 % of the total resistance, depending on displacement. Investigations on laid, welded geogrids made of surface-structured, extruded flat bars (Timmers 2003) show that the portion of the crossing elements may be up to 80 % of the total resistance. A limitation of the deformations is further achieved by a high axial rigidity of the reinforcement and thus mobilization at small deformations. The following description is made possible with the mechanical approach pursued.

The inserted reinforcement hinders the development of discrete shear bands already at very small total strains due to the geogrid structure in connection with its tensile stiffness, and it increases the zone, where intergranular strains occur, up to a certain degree, but decreases the absolute amount of intergranular strains. After exceeding a soil-specific dilatant deformation, where discrete shear bands are then formed with a delay (towards the unreinforced state), the reinforcement is explicitly subject to tensile stress in the area of the shear band.

Whereas for unreinforced or single-layer reinforced soils the maximum shear stresses mostly concentrate on a continuous shear band, branched shear bands can occur for multilayer reinforced soils (Fig. 1). Thus, the shear stresses are distributed to a larger area of the soil and reinforcement (load distribution), so a larger soil zone is activated by relative displacements of the grains (dilatancy). At the same time, the reinforcement layer is stressed at several points and over a larger area and the maximum stress value of the reinforcement related to a specific load condition drops.

The mutual influence of the stress ratios geogrid/soil as a result of the interaction of product structure, product stiffness, axial rigidity and soil dilatancy and the associated impact on the shear strength of a cohesionless soil leads to an increase of the (against the main stress direction σ_1 mostly smaller) main stress σ_3 (Confining Effect Concept) (Ruiken 2013).

The impact of the reinforcement can be proven for the vertical stress of a multilayer reinforced soil (Bussert 2006, Ruiken 2013) as well as for the lateral shear. For granular soils, the impact of the reinforcement is shown, at lateral shear, in an area of $\Delta h \approx 0.2$ m above and below the reinforcement layer (confinement zone) and reduced in another, around $h \approx 0.15$ m thick soil area (transition zone) (Cook & Horvat 2014, Horvat & Klompmaker 2014, Lees 2014). Recalculations of reinforced triaxial tests (Lees 2014) show that the compensating cohesion in the reinforcement zone must be up to 50 kN/m² and on average 25 kN/m² in order to display the deformation conditions.

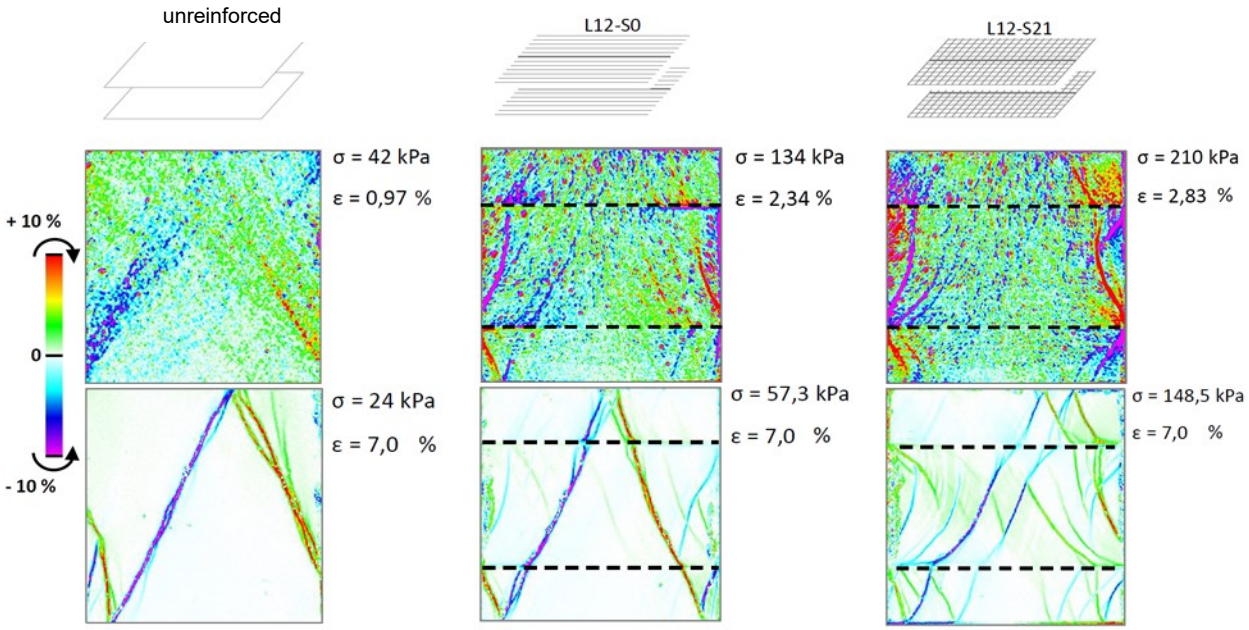

Figure 1. Distribution of shear zones depending on the proportion of cross bars with the same monoaxial compression of the specimens ε_1 in the post-fracture area (Jacobs 2015)

The overall majority of the results analysed by Vollmert (2016) on the influence of reinforcement products is based on the application of extruded, stretched biaxial geogrids and on welded biaxial geogrids laid of surface-structured, flat bars. In single cases, hexagonal products were included in the investigations, whereby the product structure did not show a better behavior compared to biaxial products (Ruiken & Ziegler 2009, Ruiken 2010). As far as systematic variations are made whereas all other test conditions and geometric properties of the reinforcement remain unchanged, the influence of the stiffness is significant with regard to the quantity.

3 SMALL-SCALED LOADING TESTS

3.1 *Test device*

To examine the fundamental factors of a geosynthetic reinforced unpaved road a small-scaled test model was set up.

A layer of soft soil (subsoil) was inserted within a testing chamber with a diameter of 50 cm (Fig. 2). On top of the soft subsoil a layer of geosynthetic was placed and then a statically compacted base course. Using a load piston (of diameter D = 5 cm), static and cyclic loading was applied. The settlements of the load piston and the deformations of the base course were monitored. Additionally, in some tests pore water pressures were measured within the soft subsoil.

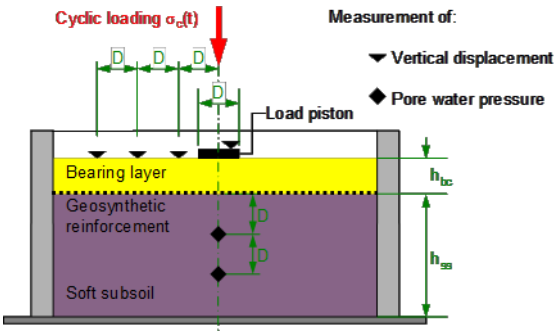

Figure 2. Setup of the model scaled loading tests

3.2 *Placement of the soft subsoil*

For each loading test the fine grained soft subsoil was mixed up and subsequently filled homogenously, without air bubbles to a minimum thickness of h_{ss} = 20 cm. The properties of the soft soil are given in Fig. 3. To facilitate placement of the subsoil the sample was mixed at a water content of 80 M.-%, roughly

twice the water content at liquid limit w_L. The high water content also limits the amount of undesired air bubbles within the soil if carefully pumped into the testing chamber.

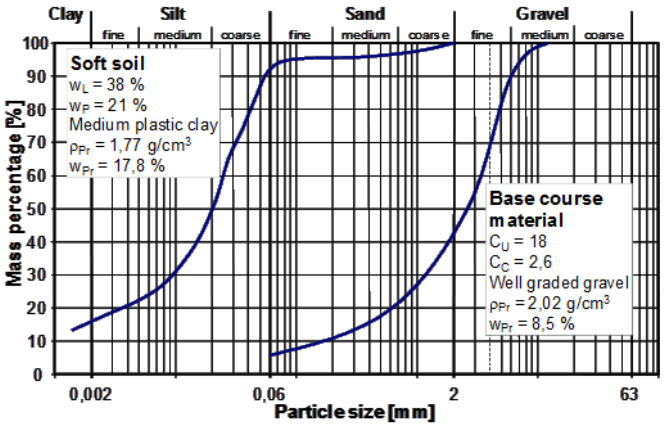

Figure 3. Soft soil and base course material used in the model scaled loading tests

In the testing chamber the subsoil was consolidated until end of primary consolidation was reached (at least about 2 days) under static load using a rigid steel plate. The consolidation stress was varied in order to obtain a certain undrained shear strength s_u. With this method it is possible to achieve a homogenous density, water content and shear strength. This was checked before the loading tests by measuring the undrained strength s_u using a small vane shear test apparatus and the water content w.

The base course material is a well-graded crushed gravel including about 7 M.-% of fines < 0.06 mm in diameter (Fig. 3). The angle of repose was found to be approximately 40 .

3.3 *Geosynthetics and base course material*

In accordance with the small-scaled loading test conditions, including geometrical and force scaling, a grid-like geosynthetic (GT-1) and a nonwoven geosynthetic (GT-2) were chosen whose mechanical strength and stiffness are considerably lower than that of geosynthetics used in field conditions (Table 1).

Table 1. Parameters of model type "Geosynthetics"

	Tensile strength [kN/m]		Elongating at failure [%]	
Direction	md	cmd	md	cmd
GT-1 (grid-like)	19.6	12.8	2.9	2.6
GT-2 (non-woven)	1.9	2.7	18.0	33.0

md: test sample cut out parallel to machine direction during manufacturing (machine direction)
cmd: test sample cut out perpendicular to machine direction during manufacturing (cross machine direction)

After consolidation of the soft soil the geosynthetic was placed firmly on top of the smooth surface of the subsoil.

The base course material (Fig. 3) was placed with a homogenous water content of w = 5 M.-%. The base course was compacted to a dry density of ρ_d = 1.85 g/cm³ by a loading plate under a defined load for 2 minutes. The short duration of the loading ensures that there is no further consolidation and thus, strength gain of the cohesive subsoil. The base course thickness was defined relative to the diameter of the loading piston and varies between 0.5 D and 1.5 D.

3.4 *Test procedure*

The main output quantity used for the evaluation of the test series was the bearing capacity of the soft subsoil alone. Hence, several tests were conducted by loading the soft subsoil without the base course material. In these tests, the undrained strength s_u of the soft soil was varied by changing the consolidation pressure. Later, experimental tests on unreinforced and reinforced bearing layers were carried out.

There were two types of loading in the model scaled tests. First, a static load with a constant rate of deformation was applied. The bearing capacity was defined as the medium stress under the loading piston, measured at a settlement of s = 20 mm or s / D = 0.4.

Figure 4. Loading on top of the surface of the base course

Second, sinusoidal cyclic loading was applied for a number of tests, with a loading stress that was varied between 5 kPa and 105 kPa at a frequency of 1 Hz. For evaluating the test results the settlement at 100,000 cycles was recorded.

3.5 *Static loading test*

As an example, the static bearing capacities q_s of the test series, where the geosynthetic GT-2 was used, are shown for different base course thicknesses of 0.5 D, 0.75 D, 1.0 D und 1.5 D, with an undrained shear strength of the soft soil between s_u = 5 kPa and 35 kPa.

The test results, depicted in Fig. 5, show that for low base course thickness (0.5 D) there is little improvement of the bearing capacity, independent of the used geosynthetic. For a base course thickness of at least 0.75 D, and especially for low subsoil strengths, the bearing capacity increases considerably. Furthermore, it can be seen that for higher shear strengths, s_u = 30 kPa and above, the increase of the bearing capacity is marginal for static loading conditions.

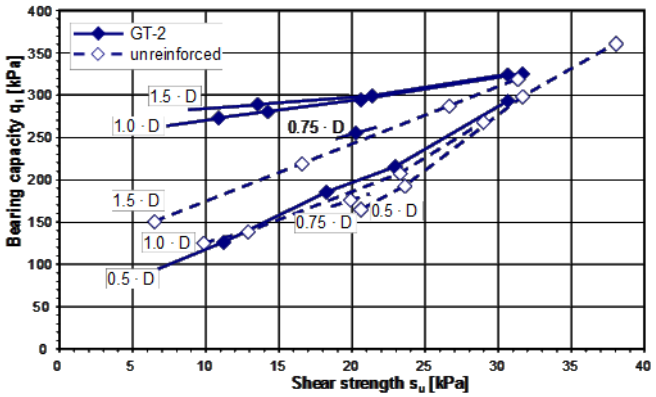

Figure 5. Results of the static loading tests featuring the geosynthetic GT-2

Table 2 shows the bearing capacity achieved, with an undrained strength of s_u = 20 kPa and a factor of strength gain due to the nonwoven geosynthetic GT-2.

3.6 *Cyclic loading test*

Exemplarily, some results of the cyclic loading test are presented here.

Table 2. Static loading, bearing capacity q_s at s_u = 20 kPa

Height of bearing layer h_{bc}	Bearing capacity q_s		
	Unrein-forced	Reinforced GT-2	Factor of increase
0.50 D	155	195	1.3
0.75 D	175	255	1.5
1.00 D	185	290	1.6
1.50 D	240	300	1.3

The application of the rigid grid-like GT-1 results in a further settlement reduction compared to the more flexible and soft nonwoven geosynthetic GT-2. The influence of the geotextile reinforcement decreases with increasing undrained subsoil strength, until approximately s_u = 30 kPa, where no further effect is visible.

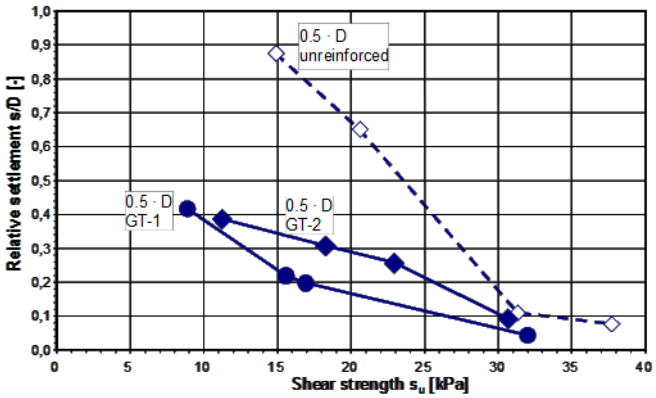

Figure 6. Relative settlement s / D of the model footing after 100,000 cycles at a base course thickness of 0.5 D

Table 3 tabulates the relative settlement s / D for a base course thickness of h_{bc} = 0.5 D and a subsoil strength of s_u = 20 kPa. At this base course thickness and subsoil strength the effectiveness of a geosynthetic layer in the model scaled test was found to be maximised. The experiments show that even usage of a low tensile strength (GT-2) geosynthetic leads to a 57 % reduction in settlements, compared to the unreinforced case. The stiffer grid-like geosynthetic GT-1 was even found to reduce the settlement by 75 %.

Table 3. Comparison of the results at su = 20 kPa, hbc = 0.5 D

System	Height of base course h_{bc}	Relative settlement s / D	Settlement reduction
unreinforced	0.5 D	0.67	-
reinforced GT-1		0.17	75 %
reinforced GT-2		0.29	57 %

4 LARGE-SCALED LOADING TESTS

4.1 *Test setup*

Figure 7 gives the test setup which is close to the situation on a typical site of an unpaved base course, which might be representative for the construction state of a road or for a temporary road. Static and cyclic loads were applied to the surface of the bearing layer by means of a circular and rigid steel plate (diameter D = 300 mm). The resulting time and cycle were recorded, as well as the varying pore pressure in the soft subsoil.

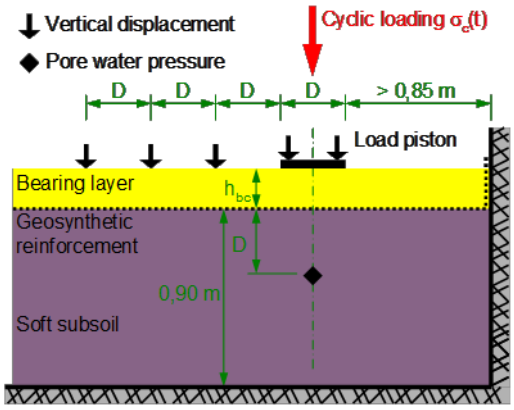

Figure 7. Large-scale static and cyclic loading tests

4.2 *Subsoil material, preparation and installation*

A low plasticity clay was used for the soft subsoil material, a by-product of a nearby plant producing aggregates for road construction. This obtained clay was found to be very homogenous, with an almost constant water content.

The clay was installed in 3 layers with a water content of 18 M.-% each compacted with a sheep foot roller (tamping roller, 1500 kg). The full thickness of the subsoil was about 0.9 m.

After compaction, the density ρ and the water content w were determined in a 1 m by 1 m grid as well as the undrained shear strength s_u (vane shear test). The tests showed a very low variation in the results from shear strength s_u and water content determination.

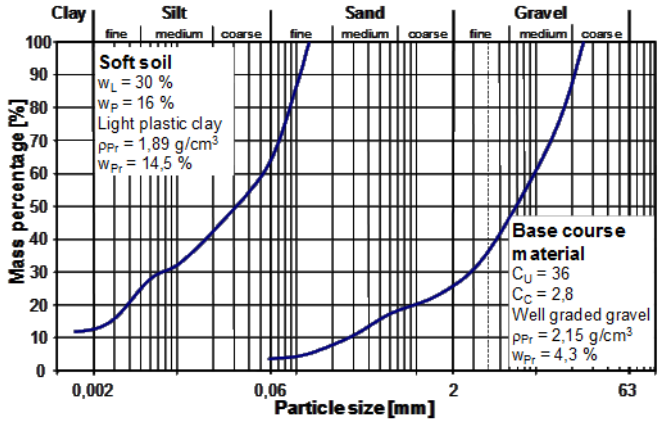

Figure 8. Soft soil and base course material used in the large scaled loading test

Figure 9. Subsoil installation for the large-scale tests

4.3 *Geosynthetics and base course material*

The reinforcement layers considered were a nonwoven (GT-3), a geogrid (GT-4) and a compound material (GT-5), consisting of the previously mentioned products (GT-3 and GT-4, Table 4).

The base course material was a well graded gravel with rounded grains that was placed to thickness from 0.5 D (150 mm) to 1.5 D (450 mm, Fig. 8). The water content of the base course was 5 M.-% for each test setup and dynamic compaction was achieved in 4 passes with a vibratory plate of 140 kg weight.

The shear strength of the compacted gravel was validated by a small series of triaxial compression tests, at a proctor density of ρ_{Pr} = 1,89, the angle of friction was found to be around or even higher than 50 .

Table 4. Parameters of geosynthetics used in large-scale tests

	Tensile strength [kN/m]		Elongating at failure [%]	
Direction	md	cmd	md	cmd
Non-woven GT-3	6.5	10.0	50	30
Geogrid GT-4	40.0	40.0	8	8
Compound material GT-5	40.0	40.0	8	8

4.4 *Cyclic loading*

Several parameters as e.g. shear strength of subsoil, relative base course height (h_{bc} = 0.5 D to 1.5 D) and cyclic loading $\sigma_{c,max}$ (350 to 550 kPa) have been varied as well as the type of reinforcement. For the last one a nonwoven, a geogrid from laid and welded bars and a compound product hereof have been used.

Since no large deformations occurred during the test, a total of 100,000 cycles were applied with a frequency of 0.3 Hz.

Figures 10 to 12 show that at a small base course thickness of h_{bc} = 0.5 D (150 mm) and a moderate loading ($\sigma_{c,max}$ = 350 kPa; Fig. 10) there is little difference between the GT-3 and GT-4 products and a significant increase in performance of all systems in comparison to the unreinforced case. Furthermore, there was a significant settlement reduction for the product GT-5.

Increasing the load ($\sigma_{c,max}$ = 450 kPa, Fig. 11) and keeping all other boundary conditions constant result in increased deformations of the compound product, GT-5 as well. Under higher loads and a low base course thickness all products can be seen to behave similarly.

Considering a loading of 450 kPa and increasing the base course thickness to h_{bc} = 1.0 D = 300mm; Fig. 12) shows again the benefit of the compound material GT-5. The difference between the other two products (GT-3 and GT-4) is negligible.

With a further increase in the cyclic loading stress of $\sigma_{c,max}$ = 550 kPa, and with the other conditions kept constant, the nonwoven (GT-3) fails after a small number of cycles. The stiffer products GT-4 und GT-5 show a better performance and similar deformations at low cycles.

A summarising graph showing the settlements at n = 1000 cycles, with the majority of test results is given in Fig. 13.

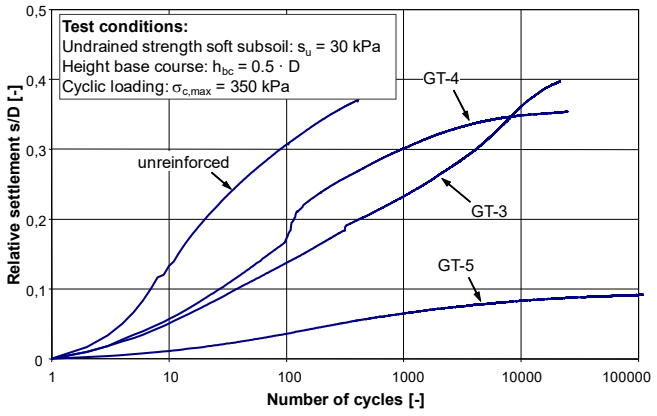

Figure 10. Cyclic loading $\sigma_{c,max}$ = 350 kPa, s_u = 30 kPa, h_{bc} = 0.5 D

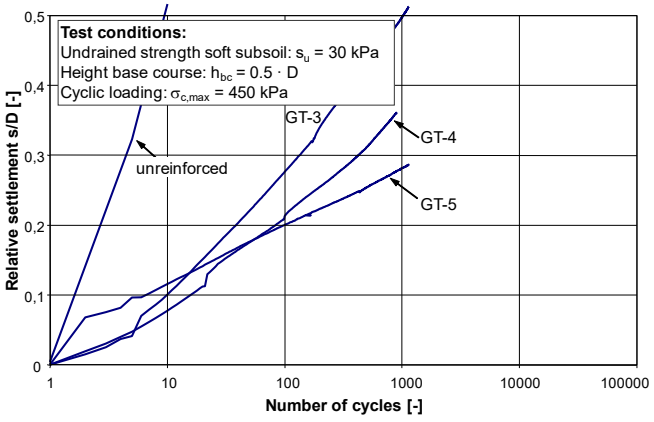

Figure 11. Cyclic loading $\sigma_{c,max}$ = 450 kPa, s_u = 30 kPa, h_{bc} = 0.5 D

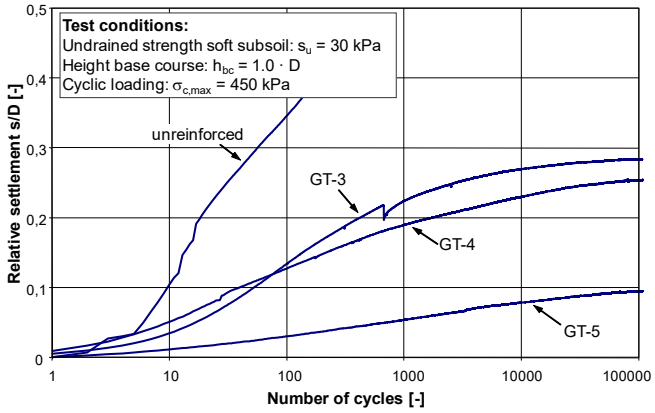

Figure 12. Cyclic loading $\sigma_{c,max}$ = 450 kPa, s_u = 30 kPa, h_{bc} = 1.0 D

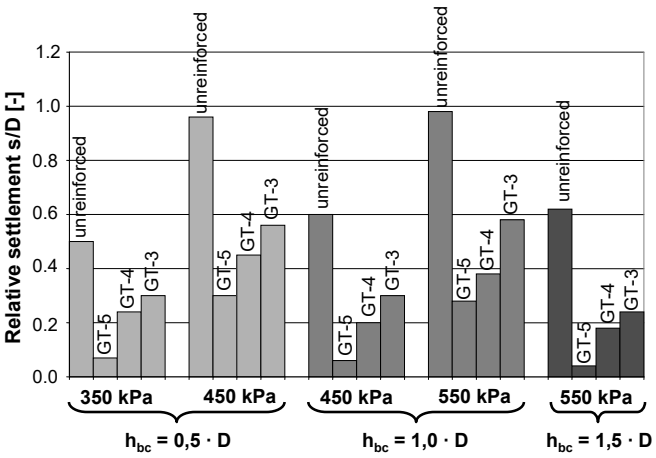

Figure 13. Summary of the relative settlements (s/D) after n = 1000 cycles with a subsoil undrained shear strength s_u = 30 kPa

5 FIELD MEASUREMENTS

By means of field measurements and recalculations at roads, the strains occurring at the reinforcement during the wheel pass and the related deformations and stresses were determined. In the following, exemplary results are presented from Vollmert (2016).

5.1 *Roads and traffic areas without bound superstructure/pavement*

To describe realistic load situations, field tests with driven wheels are chosen and preferred, compared to restraint-guided, not driven wheels under encapsulation. The chosen test is the only one (for example in contrast to cyclic plate-load tests) where all decisive load parameters are part of the investigations (Han & Vollmert 2015), especially the three-dimensional and contrary rotation of the main stress direction as well as dynamic driving influences which are known to have a significant effect depending on the extent of the deformations.

The designed and performed test fields in Tostedt with 8 test sections each were built with the following aims:

- Tostedt I: Determining the influence of the strain stiffness, multi-layer reinforcement and layer thickness of the base course according to Fig. 14.
- Tostedt II: Comparing different products used on the European market under same conditions. Emersleben et al. (2015) report about the results of this test series.

The rut depth z_N (Fig. 15) was assessed as relative rut depth in consideration of (amongst others) the initial height h_0, the CBR value of the subsoil and the number of passes.

The relative rut increase a as valuation standard shows a clear dependence on the total tensile stiffness of the installed reinforcement layers as far as the valuation is subject to nearly identical boundary conditions (Fig. 16). The positioning of the reinforcement in the base course could be identified as another decisive impact on the serviceability. Splitting the tensile stiffness to two reinforcement layers, in total a more ductile reaction of the base course was observed than for a single-layer structure at the bottom of the base course (Fig. 17) with the same sum of installed stiffness.

The strains and stresses observed in the designed structures are qualitatively very similar to those determined by Zander (2007) in the model roads of the BASt, but quantitatively higher due to the weaker subsoil conditions. The plastic strains accumulate to 0.05 % in the relatively stiff field 1.1 transverse to the trafficking direction. The rut increase (rate of rutting) decreases significantly (Fig. 18), thus documenting a stabilization of the overall structure.

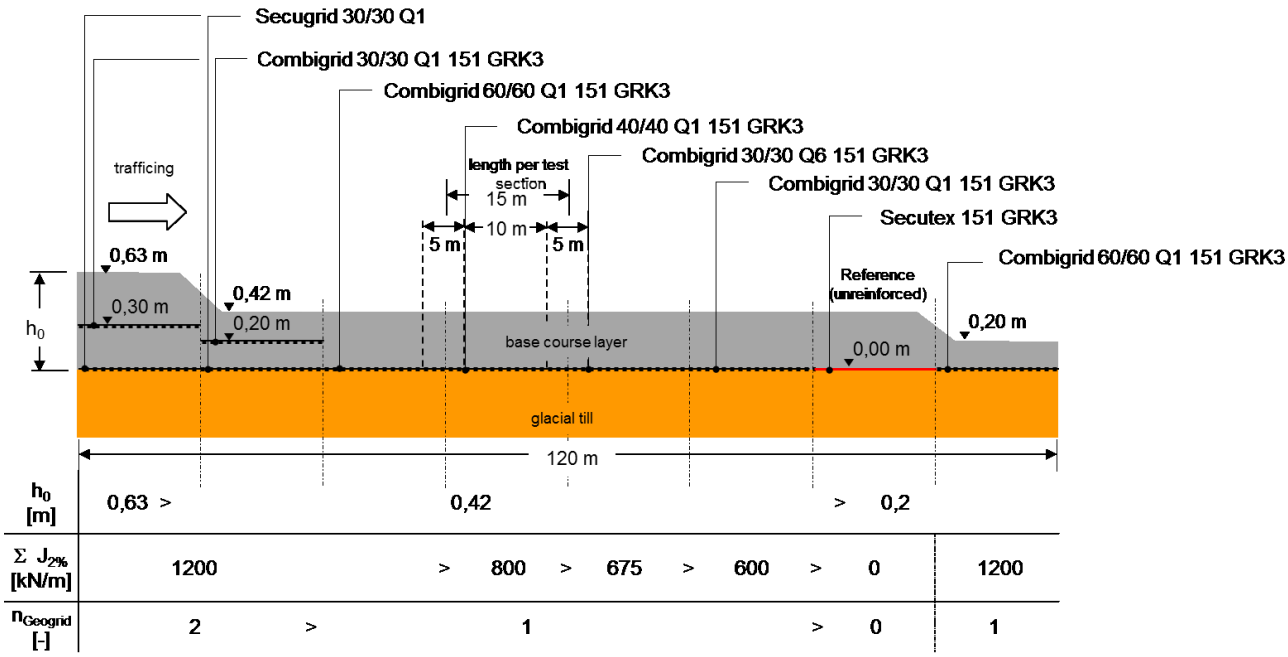

Figure 14. Longitudinal section Tostedt 1 (not to scale)

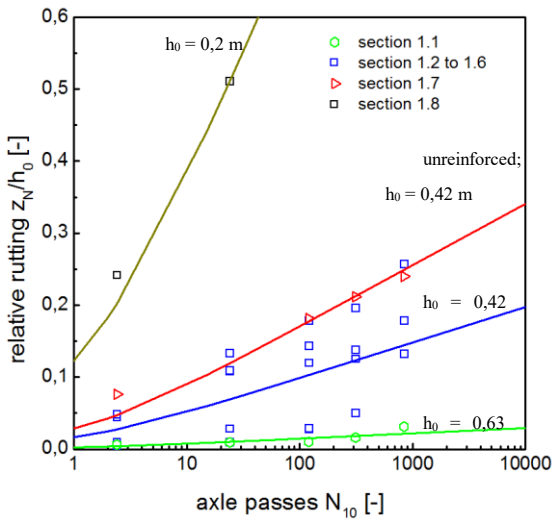

Figure 15. Development of the wheel ruts with the number of axle passes N10 for the test sections 1.1 to 1.8

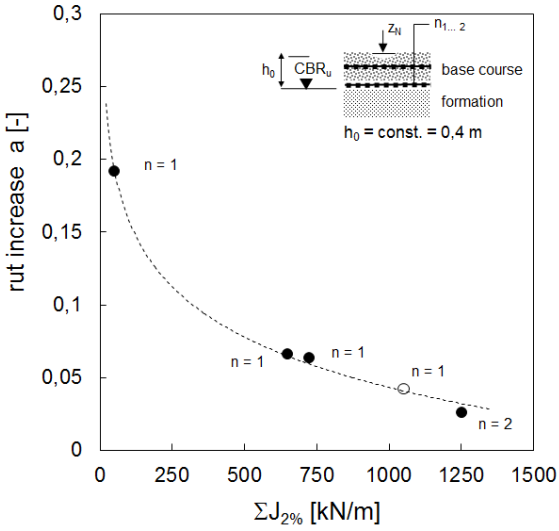

Figure 16. Rut increase a depending on the tensile stiffness J2% for the same number of axle passes N10 (a = f(CBR, h0, zN))

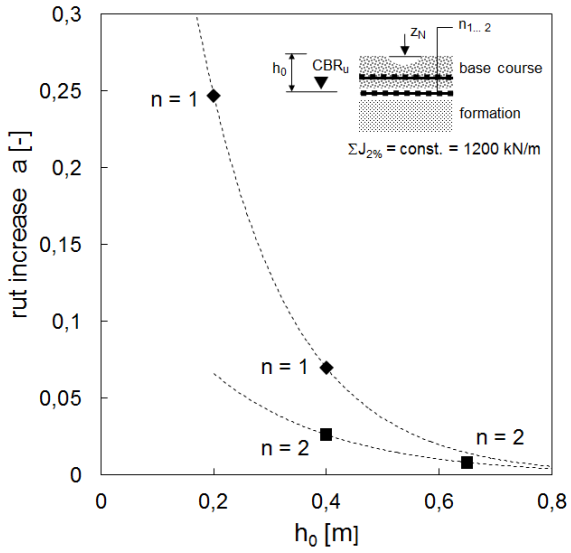

Figure 17. Rut increase a depending on the installation height h0 and the number of the reinforcement layers n at a constant sum of the installed tensile stiffness ΣJ2% = 1200 kN/m and the same number of axle passes N10 (a = f(CBR, h0, zN))

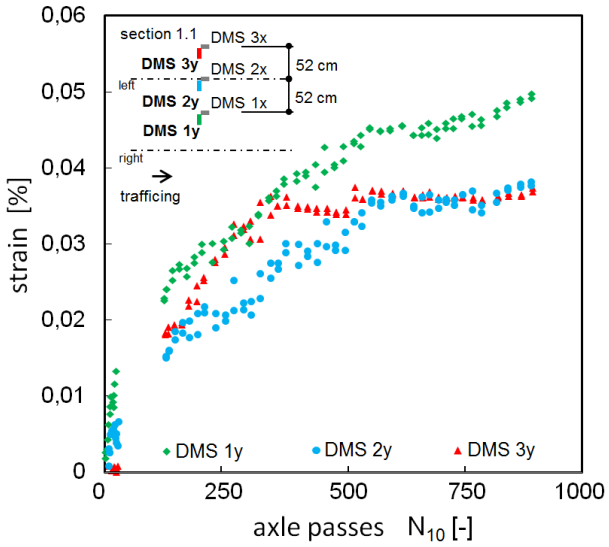

Figure 18. Geogrid strains measured by strain gauges (DMS) crosswise to trafficking direction, section 1.1

6 CYCLIC TRIAXIAL TESTS VERIFYING THE REINFORCING EFFECT

6.1 *Investigation concept*

The triaxial test was chosen as basis for the test setup (Fig. 19). This test is accepted in soil mechanics to determine material properties of soils and construction materials and allows a differentiated assessment of the test results. If an appropriate test device is used, the samples can be loaded with a high number of cycles which enables also the investigation of accumulated deformation.

The limited sample size (d = 19 cm, h = 38 cm) necessarily requires an adaptation of the grain distribution to the test facility/rig, especially of the maximum grain size. The geogrid with a geometric scale of 1 : 2.6 (Fig. 20) is matched to the grain-size distribution. The tensile strength of the sample grid is almost preserved at the scale 1:1 compared with the prototype Secugrid®30/30 Q1. Due to the dimensions preset by the test rig, the model geogrids were arranged in three layers. Altogether, 19 tests were carried out according to national and international test instructions for classified road aggregates as well as under modified conditions.

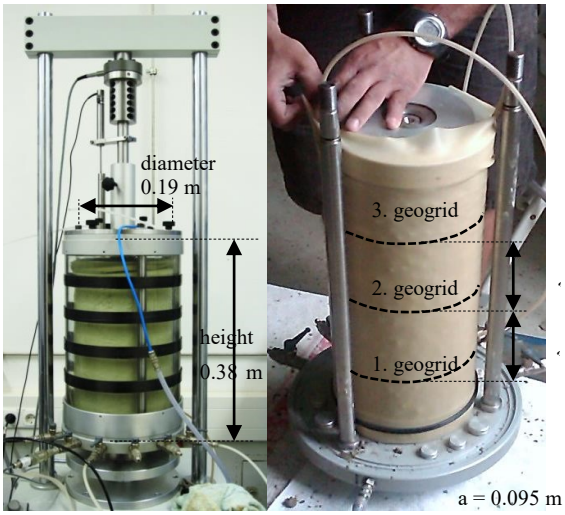

Figure 19. Triaxial test facility and placement of the samples, HTW Dresden

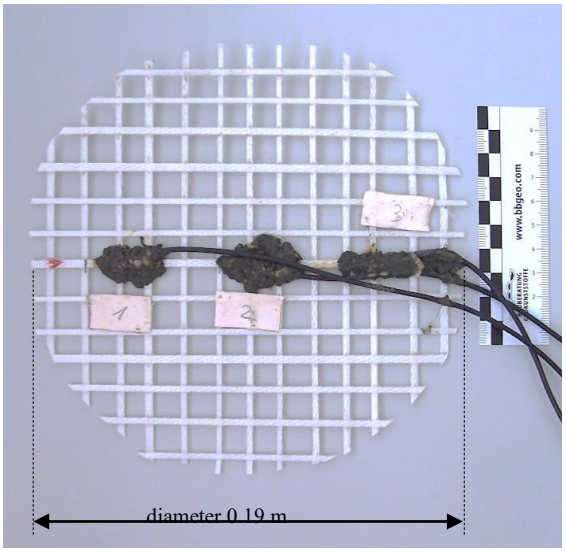

Figure 20. Geogrid Secugrid® 30/30 Q1, geometrically scaled to 1 : 2.6

6.2 *Essential results*

In a range of tests carried out according to ASTM test specification D3999 with cyclic loading, the reinforced sample has, under drained conditions, a significantly increased E-modulus compared to the unreinforced sample. The increase of the E modulus and, in analogy to this, the increase of the shear modulus is identifiable for very small deformations already (ε_1 = 0.004 %) and is between 25 % and 70 % (Fig. 21) for the maximum measured elastic strains of ε_1 = 0.25 %.

The influence of the reinforcement can be visualised with tests performed according to DIN 13286-7 with modified loads. Fig. 22 shows the development of the uniaxial compression of a reinforced and unreinforced sample, while the stress range (deviator stress), with constant lateral pressure, was increased after 10,000 load cycles each. Up to deviator stresses of 100 kN/m² the deformations stabilize in both samples on a comparable level. In case of a further increase of the stress range, visible plastic deformations occur in the unreinforced sample. They accumulate by the number of load cycles and lead to a strong compression of the sample. The strong compression of the unreinforced sample results in a premature failure compared to the reinforced sample. The compression of the sample can be compared in principle with the compaction of a base course on a very stiff ground.

The evaluation of the elastic modulus for the respective load cycles shows a strong increase of the stress absorption capacity. After a "warm-up" of the sample (increase of the strain), the sample is stabilized after 5,000 load changes each. The interesting point is that the reinforced sample shows an almost constant elasticity and a similar E modulus for all stress differences. The elastic modulus of the unreinforced sample, however, first slightly rises with increasing stress differences as a result of the compression. The unreinforced sample fails when the value of the reinforced sample is achieved.

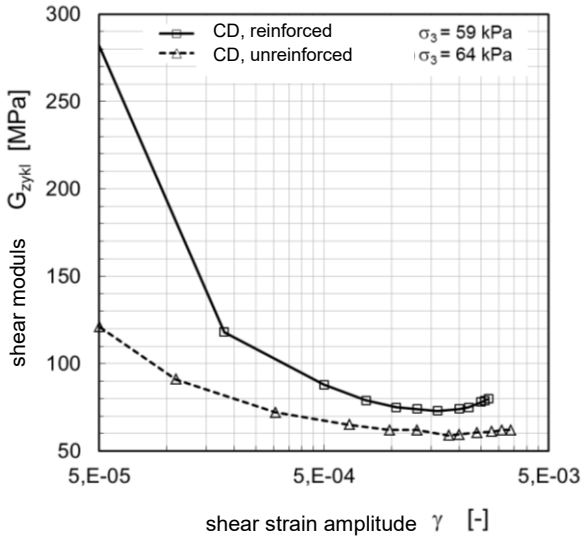

Figure 21. Application of the shear modulus via the shear strain amplitude for the reinforced and unreinforced case (ASTM D 3999-91)

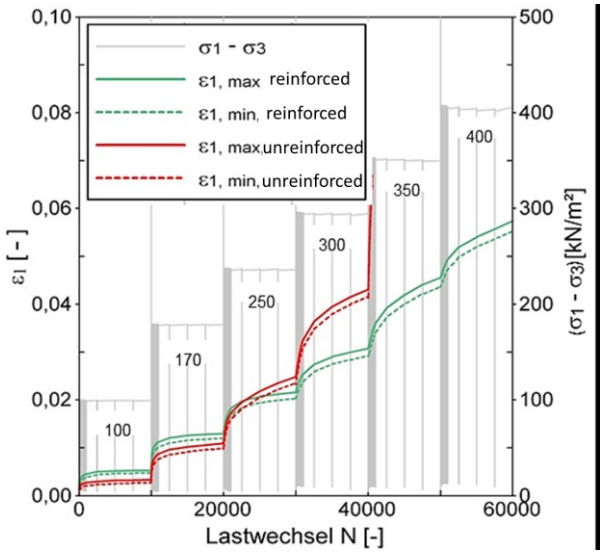

Figure 22. Comparison of the uniaxial compression of the reinforced and unreinforced sample by increasing the deviator stress after load changes of ΔN = 10,000 each (σ_3 = 45 kN/m²) (CD, DIN EN 13286-7 mod.)

7 CONCLUSION

Unpaved minor roads used for agricultural purposes and rural roads with low traffic volumes in general, as well as temporary access roads (especially for construction measures) usually consist of an unbound bearing layer of coarse-grained material. The results from the experiments both laboratory (small-scaled and large-scaled loading tests) and field tests show that the performance of the bearing layer can be improved by the use of geosynthetics. The effectiveness of the examined geosynthetics is strongly dependent on the strength of the subsoil and the thickness of the bearing layer. In the case of low subsoil strength and small bearing layer thickness, the effectiveness of geosynthetics is high. The thickness of the bearing layer, which often consists of rather costly, coarse-grained materials, sometimes even crushed materials from hard rocks, can thus be correspondingly reduced, which in particular can provide economic advantages - but also contributes to conservation of resources.

The cyclic tests show for stress differences, as they are representative for unbound base courses in road constructions, an increase of the elastic modulus and in analogy to this an increased shear modulus of the reinforced sample compared to the unreinforced sample. The increase of the material parameters appears already with very small deformations below 0.01 % uniaxial compression of the composite material and also with very small geogrid strains of approx. 0.05 %. This effect occurs more intensely if the initial deformations – which are however typical for base courses, especially as a result of loads from construction phases – are somewhat larger as it has been found from the cyclic laboratory tests.

With regard to the size and in part the absolute values, the increase of the shear modulus corresponds to the values of the field measurements (Weisemann & Vollmert, 2017). In the field measurements, it can be assumed, in addition to the actual stabilization effect of the geogrids, that for small deformations the separating and filter effects are overlapping. Thus, the overall system can be stabilized effectively. Due to the stiffening of the base course and the limitation of the deformations, the weak subsoil is subject to lower shear stress. Additionally, it can be assumed that the stiffening has a positive effect on the development of the pore water pressure and that therefore the overall stiffness measured in the field is larger than determined in lab tests.

The results show, especially when directly compared with observations and measuring results from field measurements and large-scale test series, that for each load cycle plastic deformation components have a determining influence on the system behavior.

By means of triaxial tests it can be shown that the plastic deformation is decisively reduced with geogrids. With small stress differences already and after a certain preload, hardening effects occur which can be described by means of the increased material parameter shear modulus. With larger initial deformations and higher stress differences, as they can occur with local weaknesses of the subsoil or a weakened superstructure, the positive stabilization effect of the reinforcement by limiting the plastic deformations is pronounced, as the unreinforced samples already plasticize gradually and therefore finally fail. Although the reinforced composite samples suffer plastic deformations in this case, the deformations remain low and thus allow a significantly extended serviceability. Moreover, the load ratio remains small compared to the ultimate limit state.

The effectiveness of the reinforcement results from the interaction with the base course material. Preconditions for this ideally are a high quality of the base course material, a good interaction and composite action at very small strains and a sufficiently high tensile stiffness and ultimate strength.

REFERENCES

Bräu, G. & Vogt, S. 2011. Erhöhung der Tragfähigkeit direkt befahrener Schüttungen mit Geokunststoffen - Heft 1065. Forschung Straßenbau und Straßenverkehrstechnik, Heft 1065.

Bräu, G. & Vogt, S. 2018. Field and laboratory tests on the bearing behaviour of unpaved roads reinforced by different geosynthetics. Geotechnical Engineering Journal of the SEAGS & AGSSEA Vol. 49 No. 4 December 2018.

Bussert, F. 2006. Verformungsverhalten geokunststoffbewehrter Erdstützkörper. Dissertation. Schriftenreihe des Instituts für Geotechnik und Markscheidewesen, Heft 13/2006. Clausthal-Zellerfeld: Technische Universität Clausthal.

Cook, J. & Horvat, F. 2014. Assessment of particle confinement within a mechanically stabilised layer. 10th International Conference on Geosynthetics (10ICG). Berlin, Germany: DGGT, IGS.

Cuelho, E. & Perkins, S. 2009. Field Investigation of Geosynthetics Used for Subgrade Stabilization - Final report [Montana I]. Bozeman: FHWA.

Cuelho, E., Perkins, S. & Morris, Z. 2014. Relative Operational Performance of Geosynthetics used as Subgrade Stabilization - Final report [Montana II]. Bozeman: FHWA.

Emersleben, A., Meyer, N., Beuße, M. & Vollmert, L. 2015. Ausführung und Bewertung von großmaßstäblichen Überfahrversuchen an geogitterbewehrten Tragschichten, 9. Geokunststoff-Kolloquium (S. 16). Montabaur: NAUE GmbH & Co. KG.

Han, J. & Vollmert, L. 2015. Discussion on test conditions for reinforced flexible pavements, reinforced superstructures and calibration of models. Personal communication. Delft, 1st July 2015.

Horvat, F. & Klompmaker, J. 2014. Investigation of confinement effect by using the multi-level shear box test. 10th International Conference on Geosynthetics (10ICG). Berlin, Germany: DGGT, IGS.

Jacobs, F. 2015. Verzögerung der Scherfugenbildung im Vorbruchbereich, Auswertung von biaxialen Druckversuchen. Persönliche Kommunikation vom 19.06.2015. Aachen.

Lees, A. 2014. Measurement of the geogrid confining effect. 10th International Conference on Geosynthetics (10ICG). Berlin, Germany: DGGT, IGS.

Numrich, R. 2003. Modellierung des nichtlinear-elastischen Verformungsverhaltens von Tragschichten ohne Bindemitteln. Dissertation. Fakultät Bauingenieurwesen der Technischen Universität Dresden, Dresden.

Ruiken, A. 2010. Untersuchung der Bewehrungswirkung von Geogittern anhand großmaßstäblicher Triaxialversuche. Forschungsbericht. Aachen, unveröffentlicht.
Ruiken, A. 2013. Zum Spannungs-Dehnungsverhalten des Verbundbaustoffs "geogitterbewehrter Boden". Dissertation. Rheinisch-Westfälische Technische Hochschule (RWTH), Aachen.
Ruiken, A. & Ziegler, M. 2009. Materialverhalten des Verbundbaustoffs "geogitterbewehrter Boden" aus großen triaxialen Druckversuchen. geotechnik 32 (2009) Nr. 3, 148 - 155.
Schwerdt, S., Turczynski, U. & Möllers, C. 2004. Die Anwendung von Geokunststoffen zur Verbesserung der Tragfähigkeit und zur Verringerung der Spurrinnentiefe im Erdbau des Straßenbaus - Kenntnisstandanalyse Stand 05/2004. Arbeitspapier der AG 6.4 des AK 5.2 der DGGT, Dessau. Unveröffentlicht.
Timmers, V. 2003. Interaktion von Geogittern und Füllboden, Bericht über bodenmechanische Laborversuche. Aachen: Geotechnik im Bauwesen, RWTH Aachen, unveröffentlicht.
van Gurp, C. A. P. M. and Westera, G. E. (2008). Geogrid Trial Road Base NL 2008 - Final Report for NAUE, unpublished. Apeldoorn.
Vollmert, L. 2016. Zur Gebrauchstauglichkeit geogitter-bewehrter Tragschichten unter zyklisch-dynamischen Beanspruchungen. Dissertation. TU Clausthal, 2016.
Vollmert, L., Klompmaker, J. & Emersleben, A. 2017. Performance evaluation of geogrid stabilized base courses. Proc. GeoAfrica 2017, Marrakech, Morocco, p. 814 – 824.
Weisemann, U. & Vollmert, L. 2017. Wirkung von geogitter-bewehrten Schutzschichten. Eisenbahn Ingenieur Kompendium (EIK), Verband Deutscher Eisenbahn-Ingenieure e.V. (VDEI), Frankfurt/Main
Zander, U. 2007. Grundlagen einer rechnerischen Dimensionierung des Straßenoberbaus aus Asphalt. Straße und Autobahn, 9.2007, 6.